Nishimura et al., http://www.jcb.org/cgi/content/full/jcb.201301053/DC1

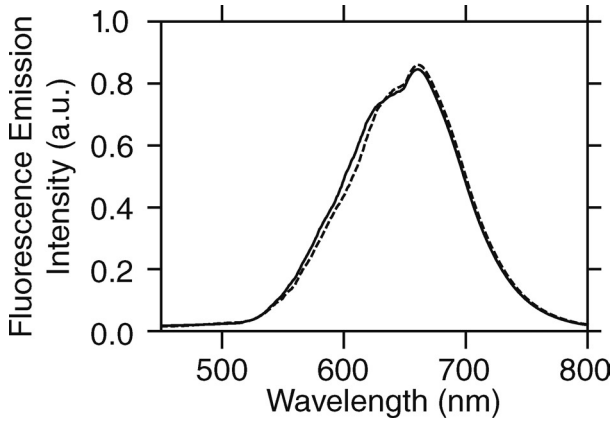

Figure S1. **The fluorescence properties of the mSiNC are not affected during storage for 60 d in dehydrated benzene.** Fluorescence spectra of mSiNC excited at 405 nm observed in dehydrated benzene. The dashed line represents the mSiNC immediately after preparation, and the solid line shows the mSiNC after 60 d of storage in dehydrated benzene at 4°C. Typical spectra among five entirely independent experiments are shown. a.u., arbitrary unit.

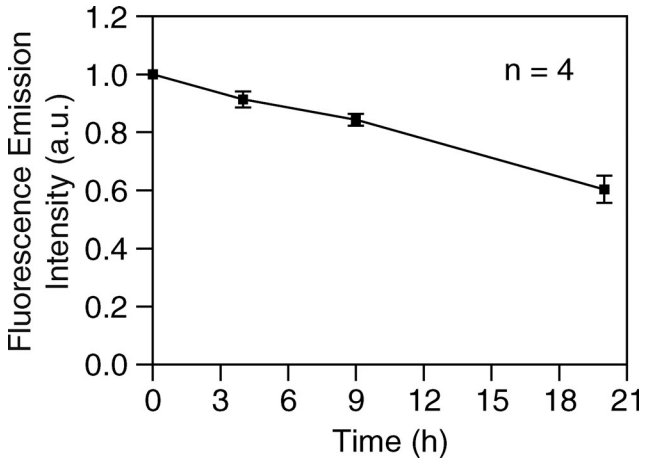

Figure S2. **Time-dependent changes of the integrated fluorescence intensity (excited at 350 nm) of the mSiNC-Tf in 50 mM phosphate buffer, pH 7.0.** The mSiNC-Tf in 50 mM phosphate buffer, pH 7.0, incubated at 4°C for 4, 9, and 20 h ($n = 4$). The fitting with a single exponential function gave $\tau_{1/e} = 42 \pm 2.8$ h (the fitting error at the 68.3% confidence limit). The bars indicate standard errors. a.u., arbitrary unit.

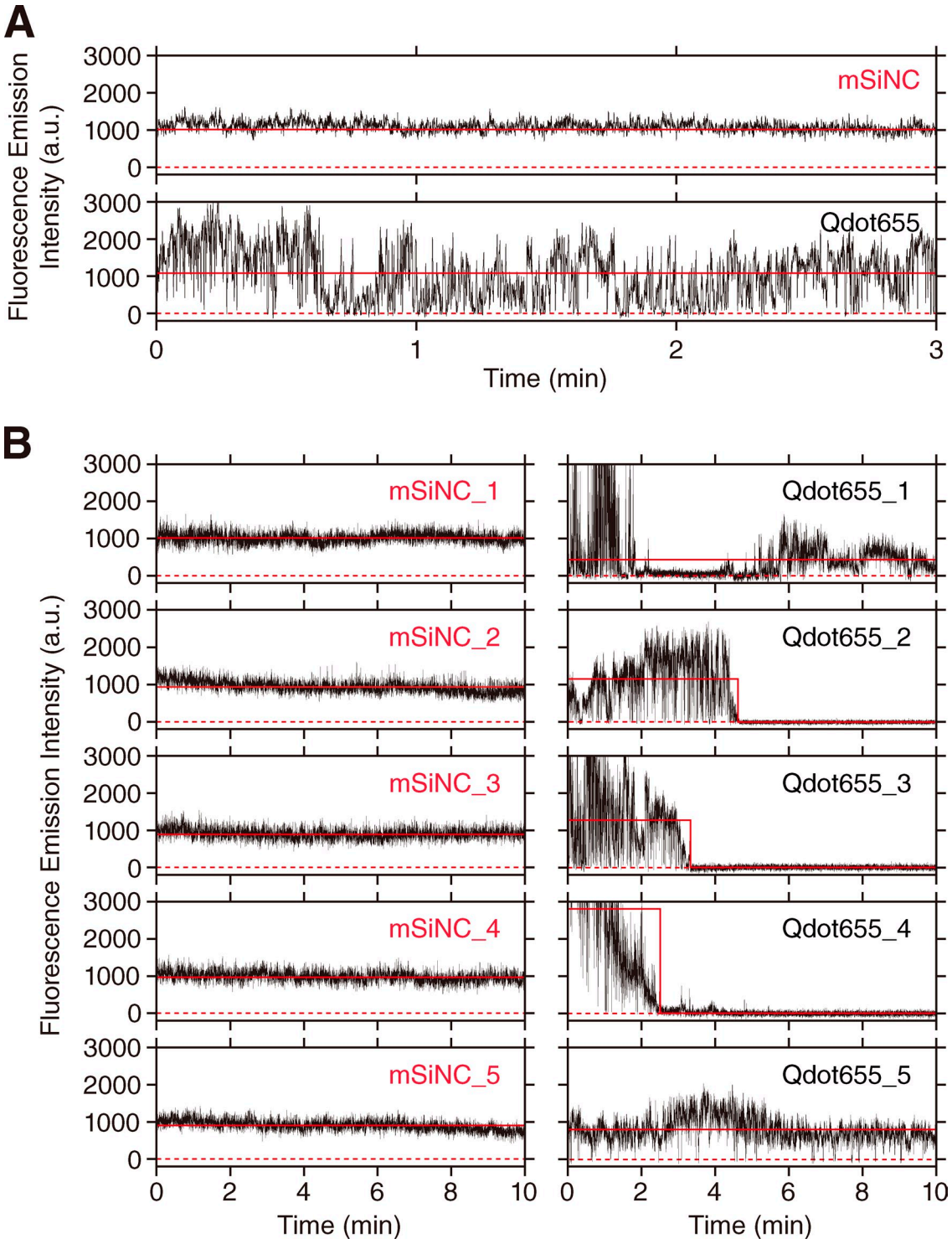

Figure S3. **mSiNC neither blinked nor photobleached, whereas QDs frequently blinked and gradually photobleached.** Typical plots of the fluorescence intensity versus time for single mSiNC and Qdot655 attached to the coverslip, observed under the same illumination (440 nm; 0.34 μW/μm^2 at the sample plane) and detection conditions, recorded at video rate (33 ms/frame; typical among 30 mSiNC and 30 Qdot655 particles, examined here. Other typical examples are shown in Fig. 4 C). Background subtraction was performed as described in the Materials and methods section (Fluorescence intensity measurements). As a result of background subtraction, the plot includes occasional negative signal intensities (0 is shown by red broken lines). The mean signal intensity is shown by red, solid, horizontal lines. Typical plots of intensity versus time for single particles, among 30 mSiNC and Qdot655 particles, examined here. Other typical examples are shown in Fig. 4 C. (A) The x axis of the plot shown in Fig. 4 C is expanded, to clarify the blinking of the Qdot655. (B) Typical time-dependent changes of the fluorescence intensities (more examples) of mSiNC spots (left) and Qdot655 spots (right). Initially, the Qdot655 is brighter, but it blinks often, and its fluorescence intensity tends to decrease greatly over time, whereas the mSiNC fluorescence is stable over the same period. Therefore, the fluorescence intensities, averaged over the duration in which the Qdot655 emits a fluorescence signal, were similar to each other, although the mean fluorescence signal intensities of Qdot655s tend to be slightly greater than those of mSiNC. Therefore, Qdot655 could be superior for short-term observations of single molecules, if blinking does not jeopardize the purpose of the experiment. a.u., arbitrary unit.

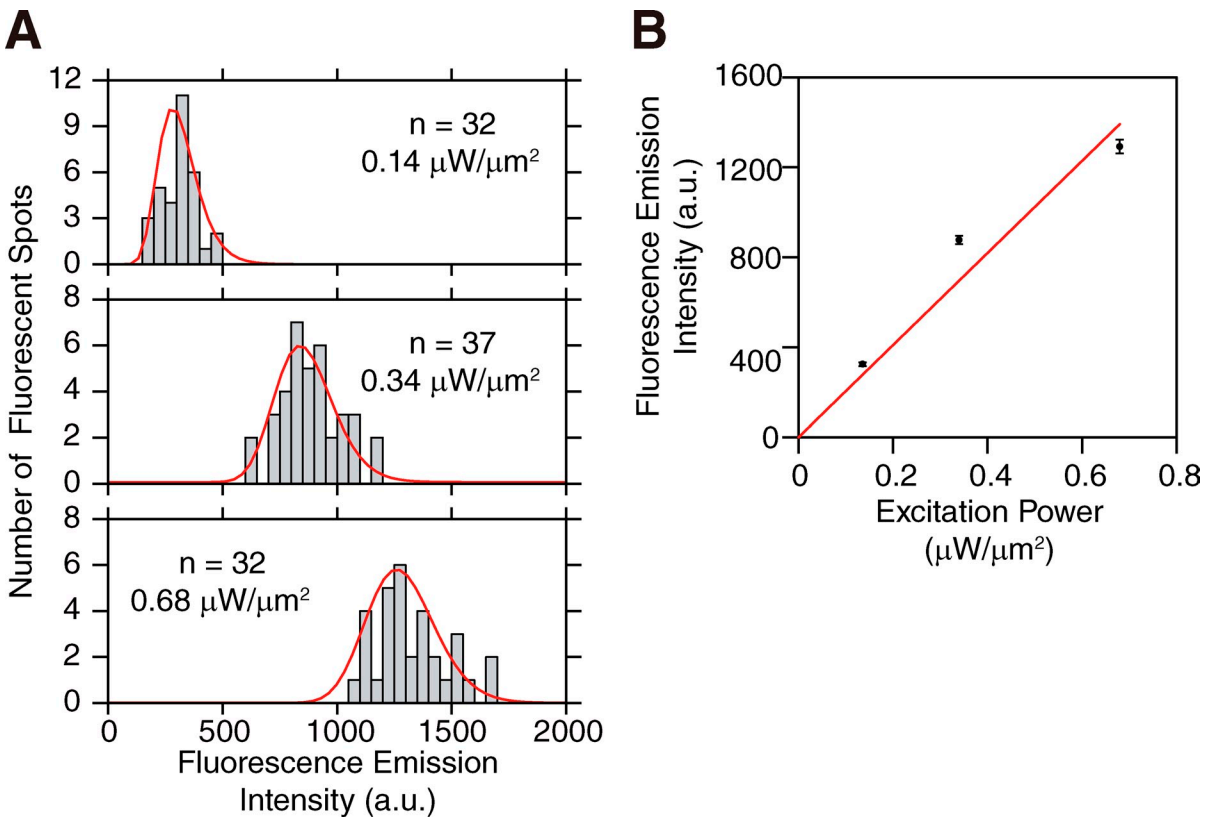

Figure S4. **Fluorescence intensity of mSiNC is linearly increased with an increase of the excitation laser intensity at least up to 0.68 μW/μm², twice the intensity generally used in the present research.** (A) Distribution of fluorescence intensities (530 × 530–nm areas) of single mSiNC excited at 440 nm with 0.14, 0.34, and 0.68 μW/μm² (after background subtraction), fitted with long-normal functions (red curves). (B) The mean fluorescence intensity determined from the log-normal fitting in A is plotted as a function of the excitation laser intensity. The plot could be well fitted by a linear function (red line). The bars indicate standard errors (*n* shown in A). a.u., arbitrary unit.

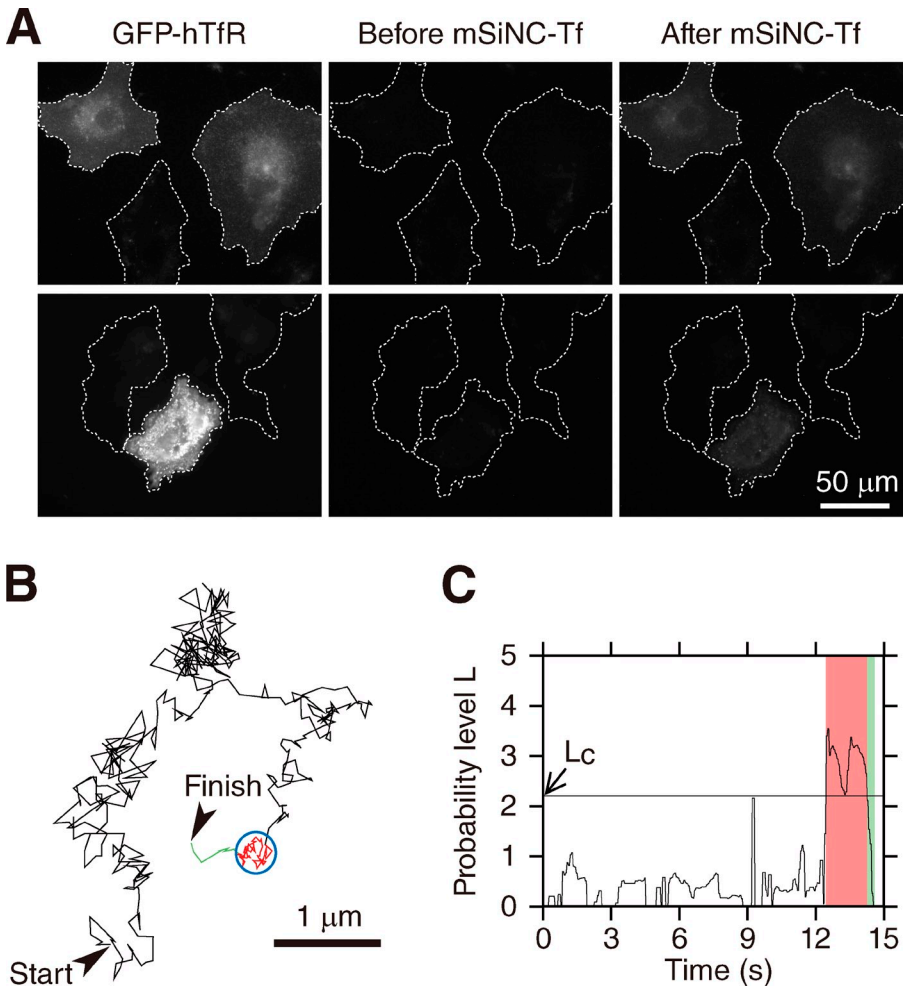

Figure S5. **Specific binding of mSiNC-Tf (human Tf) to TfR and a typical trajectory of this molecular complex (mSiNC-Tf and TfR) on the NRK cell surface including a period of temporary confinement followed by a (probable) internalization process.** (A) Representative epifluorescence microscopy images of CEF cells transfected with the cDNA for GFP-hTfR, stained with mSiNC-Tf (a view field much greater than that for Fig. 7, A and B; GFP is in the cytoplasmic domain of TfR and does not interfere with the binding of Tf to TfR). (left) A GFP image, showing that two cells among three cells shown here (cell contours shown by broken lines) express GFP-hTfR. (middle and right) An mSiNC image of the same viewfield before and after the addition of mSiNC-Tf, respectively. Only after mSiNC-Tf addition, the mSiNC-Tf fluorescence signal was detectable in only the cells that express GFP-hTfR (as shown in Fig. 7 B, mSiNC-Tf does not bind to endogenous chick TfR), showing that mSiNC-Tf binds to the chick embryonic cell surface specifically by way of the expressed hTfR. (B) A typical trajectory including a period of temporary confinement (red subtrajectory in a blue circle) followed by the (probable) internalization process of the complex of TfR and mSiNC-Tf (green trajectory; typical among 14 such trajectories). The disappearance of the signal is likely caused by the cellular transport of the endosomes out of the TIRF depth. Such trajectories occur quite frequently, although it is quite difficult at this stage to quantitatively determine the critical parameters such as the frequency of putative internalization events and residency time of the TfR in the putative coated pit. However, the trajectories that apparently involve mSiNC-Tf internalization were found systematically. Among many trajectories we obtained, we first searched for the trajectories containing at least one temporary immobilization period (using a computer program based on Simson et al., 1995) and then among them looked for those that included an immobilization period close to the end of the trajectories. In all of these trajectories, we found that the trajectories ended by short pieces of trajectories that are compatible with the concept of (apparent) directed movements or fast diffusion. These results, coupled with the established fact that TfR is internalized by way of clathrin-coated pits, strongly suggest that these trajectories represent the internalization process of TfR. (C) Statistical analysis for detecting temporary confinement, plotting the probability level *L* against time, for the trajectory shown in B. The red (green) time zone corresponds to the red (green) part of the trajectory in B.

Table S1. **Spectral properties of mSiNC, commercial organic dyes, and Qdot655**

Dye	Solvent	Abs max	Em max	φ		ε[a] (wavelength)
				Single particle	Bulk	
						$M^{-1}\ cm^{-1}$
mSiNC[b]	50 mM phosphate, pH 7.0	–	∼655	0.21	0.080	102,000 (350 nm)
						57,000 (400 nm)
						53,000 (450 nm)
Cy3[c]	PBS, pH 7.0	550	∼565	–	>0.04	150,000 (550 nm)
Cy5[c]	PBS, pH 7.0	650	∼667	–	>0.27	250,000 (650 nm)
Alexa Fluor 488[d]	PBS, pH 7.0	495	∼519	–	>0.92	71,000 (495 nm)
Alexa Fluor 594[d]	PBS, pH 7.0	590	∼617	–	>0.66	90,000 (590 nm)
Alexa Fluor 647[d]	PBS, pH 7.0	650	∼665	–	>0.33	239,000 (650 nm)
Qdot655[e] (streptavidin conjugate)	50 mM borate, pH 8.3	–	∼655	–	>0.50	9,100,000 (350 nm)
						5,700,000 (405 nm)
						2,900,000 (488 nm)
						2,100,000 (532 nm)

Bulk indicates the quantum yield determined in the bulk solution of mSiNC, whereas the number in the column of single particle indicates the quantum yield to be used in the experiments observing single mSiNC particles. This number was calculated by multiplying by 1/0.384, giving 0.21 ± 0.016 (n = 6, for completely separate preparations of mSiNC), based on the observation in which only ∼38.4% of mSiNC is fluorescent (Fig. 5). Minus signs indicate not determined. Abs, absorbance; Em, emission.

[a]The molar extinction coefficient. The brightness of a fluorescent particle/molecule is determined by the product of the molar extinction coefficient and the quantum yield (Fig. 4 C and Fig. S3). However, because of time-dependent changes, this was not applicable to Qdot655 (Fig. S3).

[b]This work.

[c]Mujumdar et al., 1993.

[d]Johnson and Spence, 2010.

[e]Qdot probes (Invitrogen).

Table S2. **The total number of consecutive images (frames) acquired for single particles of Qdot655, Cy3, and mSiNC before the particle became untrackable and their maximal gap in reconnection**

Dye	Target protein	Time resolution/frame time	Observed consecutive frames (maximal gap in reconnection)[a]	Reference
		ms		
mSiNC	TfR	<33	>3,600 (0 frames)	This work
Cy3	TfR	<33	≤150 (0 frames)	This work
Qdot655	AMPAR (GluR1)	33	>2,000 (25 frames = 0.83 s)	Heine et al., 2008
Qdot655	GlyR	75	>512 (?)	Ehrensperger et al., 2007
Qdot655	AMPAR (GluR1/GluR2)	<71.4	– (200 frames = 14.3 s)	Bats et al., 2007

Total number of consecutive images (frames) acquired for single particles of Qdot655, Cy3, and mSiNC before the particle became untrackable (number of observed consecutive frames, for generating a single trajectory = the length of a trajectory), reported in the literature. When the maximal gap in reconnection is described in the study, it is also listed here. These studies were selected because they report long trajectories and/or the maximal gap in reconnection. AMPAR (GluR1), α-amino-3-hydroxy-5-methyl-4-isoxazolepropionic acid receptors (glutamate receptor type 1); AMPAR (GluR2), α-amino-3-hydroxy-5-methyl-4-isoxazolepropionic acid receptors (glutamate receptor type 2); GlyR, Glycine receptor. The observation duration for a single molecule (particle) is given in terms of the number of observation frames (images), rather than in terms of the total observation time. The reason for this as well as the experimental factors that limit the observation duration are described in Materials and methods section Determining the observation durations for single particles/molecules. Minus sign indicates not determined. Question mark indicates not described.

[a]Maximal gap in reconnection: Trajectories obtained from single QDs or single organic dye molecules were often connected when the duration of the fluorescence disappearance (dark period) was under a threshold value. This threshold value is called the maximal gap in reconnection. In the tracking of mSiNC here, the reconnection frame is 0. The maximal gap in reconnection is often undescribed in the literature (Ehrensperger et al., 2007). The maximal gap in reconnection could be quite large when dealing with immobile molecules as shown in Bats et al. (2007).

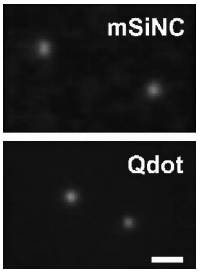

Video 1. **Fluorescence images of single mSiNCs and single QDs.** (top) mSiNCs. (bottom) QDs. Both fluorophores were adsorbed to and immobilized on polylysine-coated coverslips and were observed under a home-built objective lens–type TIRF microscope (TE2000; Plan Apochromat 60×, NA 1.49; Nikon) under the same excitation conditions (440 nm; 0.34 μW/μm^2 at the sample plane). Fluorescence images were detected by an image-intensifier (C8600-03) lens coupled to an electron bombardment CCD camera (C7190-23). Images were recorded at video rate (33 ms/frame) for 60 s (1,800 video frames) and are replayed in real time. Qdot655 blinks frequently, whereas mSiNC never blinked during the video rate observations (note that the mSiNC spots show intensity fluctuations, but the fluctuation levels are much less than those of the Qdot655s). Bar, 1 μm.

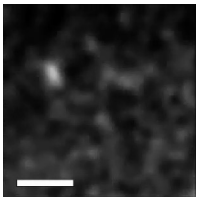

Video 2. **Individual TfR molecules each tagged with an mSiNC-Tf undergo rapid apparent simple Brownian diffusion in the plasma membrane of a live NRK cell.** The TfR molecule tagged with an mSiNC-Tf complex, observed in the bottom plasma membrane of an NRK cell. Two TfR molecules undergoing diffusion were visualized. The same image sequence is repeated twice. At the beginning of the former sequence, two TfR molecules are indicated by arrowheads. In the latter sequence, their trajectories are shown in red and yellow. Observations were performed by a home-built objective lens–type TIRF microscope (TE2000; Plan Apochromat 60×, NA 1.49; Nikon) with laser excitation at 440 nm (0.34 μW/μm^2 at the sample plane). Fluorescence images were detected by an image-intensifier (C8600-03) lens coupled to an electron bombardment CCD camera (C7190-23). Images were recorded at video rate (33 ms/frame) and are replayed in real time (because of the size limitation, only for 12 s [360 video frames]). Bar, 2 μm. The contrast of this video is lower than that of the images shown in Video 1 because the background level is high as a result of autofluorescence of the cell. This is common with living cells. The noise near the bottom part of the video frame is high because the cell is thicker there.

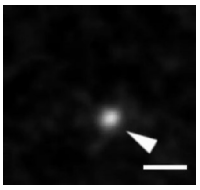

Video 3. **Direct visualization of internalization process of a TfR molecule tagged with mSiNC-Tf in the plasma membrane of a live NRK cell.** A TfR molecule bound by mSiNC-Tf, after undergoing simple Brownian diffusion (yellow trajectory), underwent temporary immobilization for 1.7 s (red trajectory and an arrowhead), probably by entrapment within a clathrin-coated pit, and then rapid movement for ~100 ms before disappearing from the TIRF illumination zone (green trajectory), likely representing internalization. Observed and played under the same conditions as Video 2. See Fig. S5 B and its legend. Bar, 1 μm.

References

Bats, C., L. Groc, and D. Choquet. 2007. The interaction between Stargazin and PSD-95 regulates AMPA receptor surface trafficking. *Neuron*. 53:719–734. http://dx.doi.org/10.1016/j.neuron.2007.01.030

Ehrensperger, M.V., C. Hanus, C. Vannier, A. Triller, and M. Dahan. 2007. Multiple association states between glycine receptors and gephyrin identified by SPT analysis. *Biophys. J.* 92:3706–3718. http://dx.doi.org/10.1529/biophysj.106.095596

Heine, M., L. Groc, R. Frischknecht, J.C. Bëïque, B. Lounis, G. Rumbaugh, R.L. Huganir, L. Cognet, and D. Choquet. 2008. Surface mobility of postsynaptic AMPARs tunes synaptic transmission. *Science*. 320:201–205. http://dx.doi.org/10.1126/science.1152089

Johnson, I., and M.T.Z. Spence, editors. 2010. The Molecular Probes Handbook: A Guide to Fluorescent Probes and Labeling Technologies. 11th edition. Live Technologies Corporation, Carlsbad, CA. 1160 pp.

Mujumdar, R.B., L.A. Ernst, S.R. Mujumdar, C.J. Lewis, and A.S. Waggoner. 1993. Cyanine dye labeling reagents: sulfoindocyanine succinimidyl esters. *Bioconjug. Chem.* 4:105–111. http://dx.doi.org/10.1021/bc00020a001

Simson, R., E.D. Sheets, and K. Jacobson. 1995. Detection of temporary lateral confinement of membrane proteins using single-particle tracking analysis. *Biophys. J.* 69:989–993. http://dx.doi.org/10.1016/S0006-3495(95)79972-6